

## Alfvén Ion-Cyclotron Instability: Its Physical Mechanism and Observation in Computer Simulation

T. Tajima, K. Mima, and J. M. Dawson

*Physics Department, University of California, Los Angeles, California 90024*

(Received 5 April 1977)

The physical mechanism of the Alfvén ion-cyclotron instability due to ion-temperature anisotropy in a high- $\beta$  plasma is explored. We have observed evidence for the proposed mechanism in runs on a magnetostatic particle simulation code. Saturation and stabilization of the instability are discussed on the basis of the present mechanism.

Since Weibel<sup>1</sup> found an electromagnetic instability in a plasma due to a temperature anisotropy (higher perpendicular temperature than parallel one), several authors have discussed similar instabilities for a plasma in a magnetic field, namely an instability for the whistler branch<sup>2</sup> and another one for the ion-cyclotron branch.<sup>3,4</sup> In a low- $\beta$  plasma the physical mechanism for these instabilities is the familiar inverse ion/electron cyclotron resonance (Landau-type).<sup>3</sup> In such a case the instability condition is universally  $T_{\perp}/T_{\parallel} > \Omega_c/(\Omega_c - \omega)$  for either electrons or ions, where  $\omega$  is the real frequency for either branch and the temperatures and gyrofrequency  $\Omega_c$  are for either electrons or ions, respectively. In a high- $\beta$  plasma, on the other hand, Davidson and Ogden<sup>4</sup> quite recently pointed out that the ion-cyclotron branch can be unstable even without the ion-cyclotron growth mechanism. Hereafter we call this instability the Alfvén ion-cyclotron (AIC) instability.

As one tries to design more efficient schemes for magnetically confined plasmas, one important measure of achievement should be the magnitude of the  $\beta$  confined. For example, recent progress in mirror experiments at the Lawrence Livermore Laboratory (2XIIIB) has prompted the design of a larger and higher- $\beta$  experiment. It is for such situations that the AIC instability draws current research attention<sup>5</sup>: This instability must be understood and stabilized. The AIC instability is dangerous especially for the mirror machine, because this instability tries to isotropize the plasma increasing the ion parallel temperature and thus can lead to the abrupt loss of confined ions. In this Letter we clarify the physical mechanism of the Alfvén ion-cyclotron instability by theoretical calculations and demonstrate that the proposed mechanism, in fact, plays a role in driving the instability by use of computer simulation. We note that our arguments apply equally

to the whistler case by exchanging the roles of the ions and electrons.

Our physical picture is based on a fluid model in which the plasma has only a  $T_{\perp}$ , and  $T_{\parallel}$  is zero; i.e., a disk distribution function—the extreme version of an anisotropic distribution. The configuration is shown in Fig. 1. When a perturbed magnetic field  $\vec{B}_{\perp}$  is applied, the ion cyclotron orbits tilt around the  $\vec{B}_{\perp}$  axis just like the tilting of a gyroscope according to  $\dot{\vec{L}} = \vec{\mu} \times \vec{B}_{\perp}$  with  $\vec{L}$  and  $\vec{\mu}$  the angular momentum and magnetic moment of a gyrating ion. In velocity space, the distribution of ions rotates around the  $\vec{B}_0 \times \vec{B}_{\perp}$  axis and this causes a parallel ion displacement and, therefore, a net current along  $\vec{B}_0 \times \vec{B}_{\perp}$ . Thus the rotation of the anisotropic distribution results in a net torque force (tensorial pressure) which enhances the parallel particle displacement more. The distinction between this mechanism and the process for the current filamentation instability<sup>6</sup> should be emphasized: In the latter case the mechanism for the instability is current-current attraction and repulsion forces (Biot-Savart interaction).

The zeroth-order ion velocity is

$$\vec{v}_{\perp 0} = \hat{x} |\vec{v}_{\perp}| \cos(\Omega t + \theta_i) - \hat{y} |\vec{v}_{\perp}| \sin(\Omega t + \theta_i), \quad (1)$$

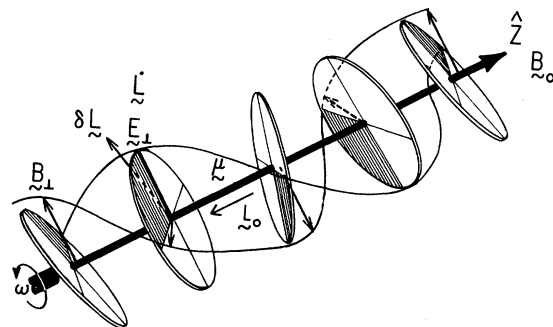


FIG. 1. Tilted anisotropic velocity distribution and the polarization of the ion-cyclotron wave.

where  $\Omega$  is the ion cyclotron frequency and  $\theta_i$  is the initial phase of the  $i$ th particle; we assume an initial uniform random distribution in  $\theta_i$ . Let us put in a perturbed electromagnetic field of left-circular polarization:  $\vec{E}_\perp = \hat{x}E_\perp \cos(kz - \omega t) + \hat{y}E_\perp \sin(kz - \omega t)$ . The equation of motion in the parallel direction  $d\vec{v}_\parallel/dt = (e/Mc)(\vec{v}_\perp \times \vec{B}_\perp)$  yields the solution

$$v_\parallel = \frac{eE_\perp}{M} \frac{|\vec{v}_\perp|k}{\omega} \frac{1}{\Omega - \omega} \sin(kz + \theta_i + (\Omega - \omega)t). \quad (2)$$

Now this perturbed parallel velocity leads to an additional force on the ion fluid in the perpendicular direction:

$$\frac{d\vec{v}_\perp}{dt} = \frac{e}{M} \vec{E}_\perp + \frac{e}{Mc} \vec{v}_\perp \times \vec{B}_0 - \frac{1}{nM} \left( \frac{\partial P_{zx}}{\partial z} \hat{x} + \frac{\partial P_{zy}}{\partial z} \hat{y} \right), \quad (3)$$

where  $P_{zx}/nM = \langle v_\parallel v_{\perp 0x} \rangle$  and  $P_{zy}/nM = \langle v_\parallel v_{\perp 0y} \rangle$ . The average is taken over initial  $v_\parallel$ ,  $v_\perp$ , and phase,  $\theta_i$ , distributions. The third term on the right-hand side of Eq. (3) is a net force generated by the stress tensor associated with the tilted nonspherical distribution function  $f(v_\perp v_\parallel)$ ; for a spherical distribution, such a term vanishes. Since the distribution of  $\theta_i$  is uniform, we obtain the tilting forces from Eqs. (1) and (2) as

$$\frac{P_{zx}}{nM} = \frac{eE_\perp k |\vec{v}_\perp|^2}{M\omega(\Omega - \omega)} \langle \sin(kz + \theta_i + (\Omega - \omega)t) \cos(\Omega t + \theta_i) \rangle = \frac{1}{2} \frac{eE_\perp k |\vec{v}_\perp|^2}{M\omega(\Omega - \omega)} \sin(kz - \omega t), \quad (4)$$

and similar expression for  $P_{zy}$ . Accordingly, Eq. (3) becomes

$$\delta\vec{v}_\perp = \hat{x} \frac{eE_\perp}{M(\Omega - \omega)} \left[ 1 - \frac{1}{2} \frac{k^2 |\vec{v}_\perp|^2}{\omega(\Omega - \omega)} \right] \sin(kz - \omega t) - \hat{y} \frac{eE_\perp}{M(\Omega - \omega)} \left[ 1 - \frac{1}{2} \frac{k^2 |\vec{v}_\perp|^2}{\omega(\Omega - \omega)} \right] \cos(kz - \omega t). \quad (5)$$

The anisotropy effectively modifies the field  $\vec{E}_\perp$  by a factor  $1 - \frac{1}{2} k^2 |\vec{v}_\perp|^2 / \omega(\Omega - \omega)$ . Substituting the perturbed ion current  $\vec{J} = n_0 e \delta\vec{v}_\perp$ , with  $\delta\vec{v}_\perp$  given by Eq. (5), and the electron drift current into Maxwell's equation, we can reproduce the dispersion relation for the AIC mode<sup>4</sup>:

$$-k^2 c^2 - \omega_{pe}^2 \frac{\omega}{\Omega_e} + \omega_{pi}^2 \frac{\omega}{\Omega - \omega} \left[ 1 - \frac{1}{2} \frac{k^2 |\vec{v}_\perp|^2}{\omega(\Omega - \omega)} \right] = 0. \quad (6)$$

The destabilizing term originating from Eq. (4) arose clearly from the noncanceling net force due to the tilted nonspherical distribution.

If the physical mechanism is based on "macroscopic" plasma motion, such plasma behavior should be able to be detected in an "experimental" measurement. In order to "see" the above physical process, we have used the 1-2/2D (three velocity and one space coordinate) magnetostatic particle code<sup>7</sup> to simulate it. In the runs we chose the following parameters:  $\Omega_e = \frac{1}{2} \omega_{pe}$ ,  $M/m_e = 5$ ,  $c = 12\Delta \omega_{pe}^{-1}$ , where  $\Delta$  is the grid spacing,  $v_{Te} = 0.6\Delta \omega_{pe}^{-1}$ ,  $v_i^\parallel = 0.25v_i^\perp$ ,  $T_e = T_i^\parallel$ , the system length  $L = 512\Delta$ , and the number of electrons and ions were 5120 each. The value of  $\beta$  for the perpendicular ion temperature was 0.32. The static magnetic field is taken parallel to the direction of spatial variation ( $\hat{z}$ ). We expected that with such strong temperature anisotropy the AIC instability will arise, and with these settings the code showed an instability. More details of the identification of this instability as the Alfvén ion-cyclo-

tron instability in thermal runs will be given elsewhere.<sup>8</sup>

To clearly extract the tilted rotation of the disk-like distribution function, we launched during a very short period a small-amplitude pilot wave of mode 4, which is the most unstable mode. We made sure that the launching was so weak that it did not destroy the linear property, but yet strong enough to favor the growth of the wave number so as to overwhelm other modes: The initial level of wave 4 is  $\sim 10$  times the thermal level of other modes. Let the perturbed magnetic field with wave number  $k$  be  $B_x = B_\perp \sin(kz - \omega t + \alpha)$ , with  $\alpha$ , the initial phase. For the ion-cyclotron wave the phase  $\chi$  defined below should decrease in time:

$$\chi = \tan^{-1} [B_{xr}(k)/B_{yr}(k)] = -\omega t + \alpha, \quad (7)$$

where  $B_{xr}(k)$  and  $B_{yr}(k)$  are the real parts of the Fourier transforms of the magnetic field in the  $x$  and  $y$  directions.<sup>9</sup> The measured wave phase is

shown in Fig. 2(a). As the wave grows well above the thermal level, the trend to monotonically decreasing phase is evident. We measure the temporal behavior of the ion distribution at a fixed spatial point. This may be done by storing test-particle velocity information around  $z = z_0$ . According to our physical picture described above, the averaged ratio of the parallel velocity to the perpendicular is given as

$$\left\langle \frac{v_{\parallel}}{v_{\perp}} \right\rangle = -\frac{eB_{\perp}}{Mc} \frac{1}{\Omega - \omega} [\langle \tan(\Omega t + \theta_i) \rangle \cos(kz_0 + \alpha - \omega t) + \sin(kz_0 + \alpha - \omega t)] = -\frac{eB_{\perp}}{Mc} \frac{1}{\Omega - \omega} \sin(kz_0 + \alpha - \omega t), \quad (8)$$

and similar expression holds for  $\langle v_{\parallel}/v_y \rangle$  at  $z = z_0$ . To derive Eq. (8), we note that the average of a periodic function with a uniform distribution in  $\theta_i$  over a period  $2\pi$  is zero. The angles of the disk rotation projected on the  $x$ - $z$  plane and the  $y$ - $z$  plane are, respectively,

$$\langle \varphi_1 \rangle \cong -\bar{\varphi} \sin(kz_0 + \alpha - \omega t), \quad (9)$$

$$\langle \varphi_2 \rangle \cong -\bar{\varphi} \cos(kz_0 + \alpha - \omega t), \quad (10)$$

where  $\bar{\varphi} \equiv (B_{\perp}/B_0)(1 - \omega/\Omega)^{-1} \ll 1$  was assumed. From Eqs. (9) and (10), the projection of tilting angles  $\langle \varphi_i \rangle$  should oscillate around zero and the amplitude of phase oscillation should grow exponentially as the wave is linearly unstable. The phase of the phase oscillation of  $\langle \varphi_1 \rangle$  should be advanced  $90^\circ$  over that of  $\langle \varphi_2 \rangle$ . The frequency of

the oscillations should be the same as the real frequency of the unstable wave. To sum up, the disk phase propagates helically with the same phase velocity as the wave and the tilting angle increases exponentially until the instability saturates.

Figure 2(b) shows the measured projected angles of the disk tilting in time. The statistical averages are made over 200 test particles located initially in the interval of  $z = (256\Delta, 266\Delta)$ . In order to avoid the singular property of the tangent in Eq. (8) and to obtain reasonable statistics<sup>8</sup> in Eqs. (9) and (10), we took the arctangent of  $v_{\parallel}/v_x$  first and then averaged over all the test particles. We see clearly the disk rotation in Fig. 2(b). First of all, the angles oscillate around zero with period  $\sim 90\omega_{pe}^{-1}$ . The theoretical period of the unstable wave is  $T = 2\pi/\omega \sim 2\pi/0.070 = 89.8\omega_{pe}^{-1}$ . Secondly, the amplitudes of the angles  $\langle \varphi_i \rangle$  increase approximately exponentially. In the third place, the phase of  $\langle \varphi_1 \rangle$  is advanced over that of  $\langle \varphi_2 \rangle$  by approximately  $25\omega_{pe}^{-1}$ , which corresponds to  $\sim 100^\circ$  phase difference as compared to the theoretical value of  $90^\circ$ . These findings in the simulation strongly support our picture of the physical mechanism.

Finally, we discuss saturation and stabilization. Until  $t \sim 200\omega_{pe}^{-1}$  the population of resonant particles is small, because the resonant phase velocity  $(\Omega - \omega)/k_{\parallel}$  for mode 4 is about  $1.4(T_{\parallel}/M)^{1/2}$ . This is another reason why we can see the disk motion in these runs: The bulk of the distribution follows the macroscopic rotation, while a small number of resonant particles should follow more complicated individual orbits. The upper boundary to the unstable wave number  $k_s$  at saturation decreases in time according to  $\Omega - \omega_{k_s} = \Omega T_{\parallel}(t)/T_{\perp}(t)$  (see Fig. 3). This is because the instability is kinetic near the upper boundary: Modes of larger  $k$  saturate quickly due to enhanced parallel temperature. After  $250\omega_{pe}^{-1}$ , the surviving modes 2, 3, and 4 with  $\omega \sim kV_A$  seem to cause small-amplitude oscillation seen in Fig. 3(b), whose period is  $120\omega_{pe}^{-1}$ , as compared with theoretical value of  $123\omega_{pe}^{-1}$  for magnetic trapping.

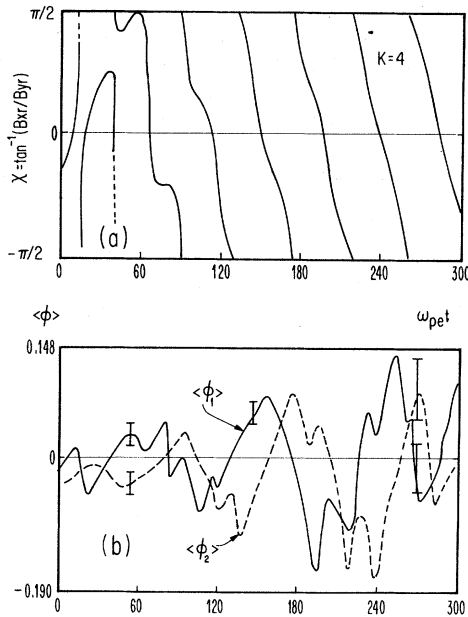


FIG. 2. Temporal behavior of phases of (a) the wave and (b) the disk tilting. The phase slippage between the two can be explained, because the wave is growing. With growth rate  $\gamma$ , the phase difference is  $\sin(kz_0 + \beta) = 0.54$ , where  $\sin\beta \equiv \gamma/[\omega - \Omega)^2 + \gamma^2]^{-1/2}$  and measured values  $\gamma = 0.11\Omega$  and  $z_0 = 260.5$  at  $t = 150\omega_{pe}^{-1}$ . Since  $\chi \sim 0$  at  $t = 150\omega_{pe}^{-1}$  in (a),  $\langle \varphi_i \rangle$  should be 0.54 times of its peak value, while (b) gives  $\sim 0.7$ .

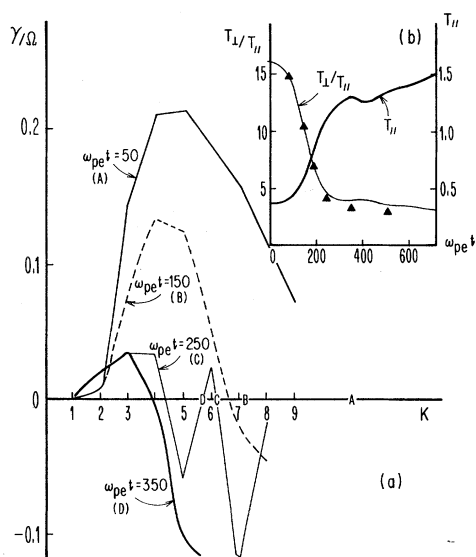


FIG. 3. Saturation of the instability and quasilinear heating. (a) Points A, B, C, and D represent the upper wave number  $k_s$  of saturation by theory for the respective time. Wave energy accumulates at lower  $k$  modes. (b) The temperature follows the quasilinear relaxation (theory in  $\Delta$ ).

These findings lead to an important consequence that we only need to stabilize the low- $k$  modes (hydro-regime). In a high- $\beta$  plasma, the longitudinal nonuniformity of  $T_{\perp}$  is the most conspicuous mechanism for the AIC stabilization.<sup>8</sup> When  $kL \lesssim 2\pi$  with a characteristic length  $L$  of the nonuniformity,  $T_{\perp}$  nonuniformity effectively reduces the tensorial pressure in Eq. (4) by a factor  $kL/2\pi$ , which is a ratio of the length occupied by hot ions to that by the wave packet. Thus in the nonuniform system we obtain increased critical  $k_c$ , the lowest possible wavenumber for which the

AIC wave is unstable, is obtained by replacing  $|\tilde{v}_{\perp}|^2$  in Eq. (6) by  $|\tilde{v}_{\perp}|^2 kL/2\pi$ . When the increased  $k_c$  decreases the critical resonance velocity  $V_{RC} = (\Omega - \omega_{k_c})/k_c$  down to the parallel thermal velocity  $v_{\parallel}$ , the phase mixing of the tilted disk rotation results, and leads to stabilization. The condition  $V_{RC} = v_{\parallel}$  yields a scaling law for the critical stabilizing length  $L_c$  of nonuniformity as

$$L_c \cong 2\pi^2 \beta^{-1/2} (T_{\parallel}/T_{\perp})^{1/2} c / \omega_{pi}. \quad (11)$$

One of the authors (T.T.) acknowledges useful discussion with Dr. J. Byers and Dr. D. Baldwin at the Q-Enhancement Conference held at the Lawrence Livermore Laboratory. The authors also thank Dr. T. Kamimura for discussions. This study was supported by Electric Power Research Institute Grant No. RP270-0-0 and National Science Foundation Grant No. PHY75-07809.

<sup>1</sup>E. S. Weibel, Phys. Rev. Lett. **2**, 83 (1959).

<sup>2</sup>R. N. Sudan, Phys. Fluids **6**, 57 (1963).

<sup>3</sup>J. E. Scharer and A. W. Trivelpiece, Phys. Fluids **10**, 591 (1967).

<sup>4</sup>R. C. Davidson and J. M. Ogden, Phys. Fluids **18**, 1045 (1975).

<sup>5</sup>D. E. Baldwin, H. L. Berk, J. A. Byers, R. H. Cohen, T. A. Cutler, L. L. Lodestro, N. Maron, L. D. Pearlstein, M. E. Rensink, T. D. Rognlien, J. J. Stewart, D. C. Watson, and M. J. Gerver, Lawrence Livermore Laboratory Report No. UCID-17038 (to be published).

<sup>6</sup>K. Molvig, G. Benford, and N. C. Condit, Jr., to be published.

<sup>7</sup>J. Busnardo-Neto, P. L. Pritchett, A. T. Lin, and J. M. Dawson, J. Comput. Phys. **23**, 300 (1977).

<sup>8</sup>To be reported in a more length paper.

<sup>9</sup>In the code the electron charge is taken positive for historical reason.